



# Innovative ceramic pigments from recycled lithium-ion battery cathodes for inkjet applications

Marta Rodrigo <sup>\*</sup>, María Fernanda Gazulla, Eulalia Zumaquero, Jorge González

*Instituto de Tecnología Cerámica (ITC), Asociación de Investigación de Las Industrias Cerámicas (AICE), Campus Universitario Riu Sec. Edificio ITC, Castellón, Spain*

## ARTICLE INFO

Handling Editor: Jens Guenster

### Keywords:

Spent lithium-ion battery  
Ceramic pigments  
Critical raw materials

## ABSTRACT

The booming of the electric mobility together with the need of storing renewable energies have increased the demand of lithium-ion batteries which will bring about increasing amounts of electronic waste. Besides, the need for alternative sources of certain raw materials considered critical has changed the perception of determined wastes, which are no longer considered residues but sources of raw materials. In this work, the active cathode material present in end-of-life lithium-ion batteries (Ni, Co, and Mn) was used as secondary raw material, after being properly separated, in the synthesis of a cobalt iron nickel manganese chromium black spinel ((Co, Fe, Ni, Mn) (Fe,Cr)<sub>2</sub>O<sub>4</sub>). The pigment was used in the formulation of a ceramic inkjet ink which was deposited over a single-fired porous tile and porcelain tile. Texture and brightness of the ink were not affected by the use of this waste, thus presenting excellent prospects for the industrial ceramic application.

## 1. Introduction

Ceramic pigments are important additive materials used for decorating products as well as supporting other properties of the obtained ceramic products. The colour or shade of the ceramic pigment is always derived from the chemical compounds of transition elements, such as vanadium, iron, cobalt, manganese, nickel, copper, chromium, praseodymium, etc [1]. They are considered the most expensive material in the ceramic tile manufacture despite being used in small proportions relative to the total mass of the product. The reason for being such a costly material is mainly because these transition elements needed to develop the colouring properties are expensive, and because of that ceramic industry is focusing research on the development of pigments with alternative raw materials [2].

Ceramic pigment industry account for a consumption of approximately 5600 ton/year of CoO, worthing about 3.5 % in terms of global demand of cobalt. Nickel consumption for the ceramic industry is estimated in more than 800 ton/year, which stands for a 0.6 %. Although this consumption is not very high in terms of global demand, the increase in its demand due to battery manufacturing could affect the supply in other sectors, such as the ceramic, and also the cost of acquisition. Regarding manganese, its consumption in the ceramic industry is around 2000 ton/year, also negligible compared to the global consumption, but also important as its use in the battery industry could

bring about supply problems [3,4].

These raw materials are also used in the manufacturing of Li-ion batteries whose demand is increasing exponentially due to the need of storing renewable energies, the increase in the demand for portable devices, and mainly, the immersion in an electric-vehicle revolution to reach full decarbonization.

The European Commission launched in 2008 the European Raw Materials Initiative whose main action is establishing a list of Critical Raw Materials (CRMs) at the UE level. The reasons for a raw material to appear in this list are for both economic importance and supply risk. This list is updated every 3 years. The first CRM list appeared in 2011 where Co was already included. Li appeared in the 2020 list for the first time because, with the increase of electric vehicle batteries and energy storage, the EU will need up to 18 times more lithium in 2030 and almost 60 times more in 2050, and this increase in demand may lead to supply issues if not addressed [5]. In 2023, a fifth list of 34 CRMs was published in Annex II of a Regulation proposal to establish a framework for ensuring a secure and sustainable supply of critical raw materials [6]. In this list, manganese becomes critical due to its supply risk increase as the result of the decrease in the domestic supply from Bulgaria and Hungary and the increase in the import reliance from South Africa and Gabon. Additionally, nickel and copper were included in this list because, despite not being classified as critical due to adequate supply diversification, they are considered as strategic.

<sup>\*</sup> Corresponding author.

E-mail address: [marta.rodrigo@itc.uji.es](mailto:marta.rodrigo@itc.uji.es) (M. Rodrigo).

Other countries have elaborated their own list of critical materials like USA, Japan, South Korea, or Canada sharing nine materials that are considered critical between all countries, including EU: antimony, cobalt, gallium, indium, lithium, niobium, PGE/PGM, tungsten, and vanadium [7].

Li-ion batteries (LIBs) are the energy storage devices commonly used nowadays. A modern LIB consists of a cathode and an anode separated by a porous separator immersed in a non-aqueous electrolyte using  $\text{LiPF}_6$  in a mixture of ethylene carbonate (EC) and at least one linear carbonate selected from dimethyl carbonate (DMC), diethyl carbonate (DEC), or ethyl methyl carbonate (EMC) [8]. The active material used in the cathode is normally a double oxide of lithium and one or more transition metals, most commonly cobalt, nickel, and manganese. For many years, lithium cobalt oxide ( $\text{LiCoO}_2$ ) (LCO) was used as cathode active material due to its high specific energy. However, the high cost of cobalt made manufacturers change to other types of chemistries in which cobalt was substituted by other transition metals. In this manner, new materials appeared such as: lithium manganese oxide ( $\text{LiMn}_2\text{O}_4$ ) (LMO), lithium nickel manganese cobalt oxide ( $\text{LiNi}_x\text{Mn}_y\text{Co}_z\text{O}_2$ ) (NMC), lithium iron phosphate ( $\text{LiFePO}_4$ ) (LFP), lithium nickel cobalt aluminium oxide (NCA), and lithium titanate ( $\text{Li}_2\text{TiO}_3$ ) (LTO). Each of these materials confers different properties to the battery in terms of specific energy, specific power, life span, performance, safety, and cost. LCO was then substituted by NMC, with different proportions of nickel, manganese, and cobalt, and, although the market tends to the use of LFP, NMC is currently being predominant [6–11].

Global demand for Li-ion batteries is expected to soar over the next decade, with the number of GWh required increasing from about 700 GWh in 2022 to around 4.7 TWh by 2030, accounting for an increase of 27 % per year [12]. The increase in the demand for portable devices, energy storage systems, and mainly, electric vehicles will bring about an increase in the amount of electronic waste generated in the next years, and more specifically, an increase in the amount of Li-ion battery waste. The recycling of this waste will therefore be challenging. It is projected that 705,000 tons of end-of-life batteries will be disposed by 2025, a figure that should hit 9 million tons a year by 2040 [13]. So, battery waste can turn into an infinite source of raw materials if well managed.

In the last decades, the production of ceramic pigments from industrial wastes has gained increasing interest as the valorisation of a residue, that will become the raw material for another product falls in the concept of the circular economy. As previously explained, LIBs contain in their composition some valuable materials such as Co, Ni, and Mn that can be used in the synthesis of ceramic pigments, if properly recovered. This residue is particularly interesting in synthesizing ceramic black pigments because it can substitute three virgin raw materials considered critical. Moreover, the environmental advantages of using these wastes as raw materials are the inertization of highly hazardous wastes into ceramic products, mitigating their colossal environmental impact, and reducing virgin raw material consumption [14].

In a previous study undertaken by this research group, cobalt aluminate blue spinel ( $\text{CoAl}_2\text{O}_4$ ) was synthesized using cobalt oxide recovered from LCO active cathode material of spent lithium-ion batteries [15]. However, the hydrometallurgical process needed for recovering cobalt oxide from the active cathode material implies the use of a great number of chemical reagents with high toxicity and challenging to handle, resulting in processes that are environmentally unfriendly and economically unfeasible. For this reason, the direct use of the recovered cathodes in the synthesis of ceramic pigments was then studied.

In this work, the synthesis of a black ceramic pigment using NMC cathode recovered from spent lithium-ion batteries is reported, enhancing the circular economy and sustainability. To do so, a great number of disposed lithium-ion batteries were chemically analyzed and classified in terms of their cathode chemistry in a first step. This classification was followed by an automatized separation process of the cathode and a series of by-products mainly enriched with nickel and

copper. The selected ceramic pigment was then synthesized with a total substitution of CoO, NiO, and/or MnO by the recovered cathode NMC. Finally, the ceramic pigment was used in the formulation of a ceramic inkjet ink that was used in the decoration of two types of industrial single-fired ceramic tiles: porous wall and porcelain.

## 2. Experimental

### 2.1. Materials

Around 250 spent LIBs from laptops of different brands and models were used to carry out this study. Current legislation does not oblige LIB manufacturers to identify the active cathode material chemistry used, although this fact is expected to change in the coming years with the implementation of the new European Regulation 2023/1542 [16] which will force the labelling of batteries containing some general information such as the chemistry, the capacity, or the critical raw materials present in the batteries. However, until this implementation occurs, discarded batteries that are currently available do not have their active cathode material chemistry identified. So, the first step that was undertaken in this study was the manual dismantling for cathode separation and chemical determination in order to create a database of LIBs from laptops classified according to their active cathode material chemistry. Fig. 1 shows the classification obtained in the analysis of 250 spent LIBs.

This study showed that almost 40 % of the current discarded laptop batteries present an NMC chemistry. However, this percentage is expected to increase with the reduction in the use of LCO chemistry due to its cost.

For pigment synthesis, reagents shown in Table 1 were used.

In the synthesis of the black pigment with NMC cathode, the use of chromium oxide and iron oxides was also needed in order to reach the composition of the selected pigment. Besides, the use of cobalt, nickel, and manganese oxides was also needed in order to prepare the standard pigment for comparison.

For ink preparation, tripropylene glycol methyl ether, and dipropylene glycol methyl ether supplied by Univar Solutions, and synthetic polymer dispersant provided by Lubrizol, were considered as main constituents for formulating the test ceramic inkjet inks.

### 2.2. Classification, separation process and characterization of the recovered cathode

For the classification step, the spent batteries were manually dismantled, and the active cathode material was separated from the rest of the components for its chemical characterization. Lithium was analyzed by inductively coupled plasma optical emission spectrometry (ICP-OES) using an Agilent model 5100 SVDV spectrometer, fluorine was determined by ion-selective electrode (ISE) potentiometry using a

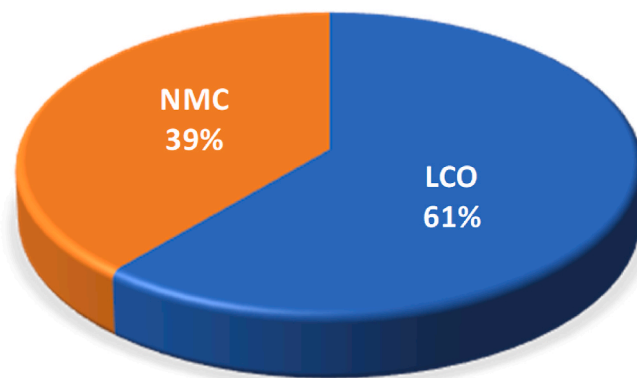


Fig. 1. Classification of discarded laptop batteries according to the chemistry of their active cathode material.

**Table 1**  
Reagents used in the synthesis of the black pigment.

| Reagent         | Formula                        | Supplier   | Purity (wt%) |
|-----------------|--------------------------------|------------|--------------|
| Cobalt Oxide    | Co <sub>3</sub> O <sub>4</sub> | Alfa-Aesar | 99.9         |
| Nickel Oxide    | NiO                            | Alfa-Aesar | 99.9         |
| Manganese Oxide | MnO <sub>2</sub>               | Fluka      | 99.5         |
| Chromium Oxide  | Cr <sub>2</sub> O <sub>3</sub> | Fluka      | 99.6         |
| Iron Oxide      | Fe <sub>2</sub> O <sub>3</sub> | Merck      | 99.9         |

Metrohm model 692 pH/Ion meter, and the rest of the major and minor components was determined by wavelength dispersive X-ray fluorescence (WD-XRF) using a PANalytical model AXIOS spectrometer. Apart from the chemical composition, the identification of crystalline structure was also determined using a BRUKER Theta-Theta model D8 Advance diffractometer. Besides, the morphology of the cathode particles was studied using a scanning electron microscope (SEM) using a FEG-ESEM Quattro S from Thermo Fisher.

With these results, a database with the lithium-ion batteries classified by the cathode chemistry used in their cells was obtained. This classification was necessary in the subsequent separation process to select those with an NMC chemistry [17].

The current separation technologies are based on dismantling and shredding processes to obtain the so-called “blackmass”, which is composed of the anode and cathode active materials and some contamination coming from the collectors, shells, etc. This “blackmass” cannot be directly used as secondary raw material in other processes without being submitted to a hydrometallurgical process, with the concerns this process presents. For this reason, an automatic separation process capable of separating the active cathode material from the rest of the components was designed and patented. This separation process involves a first cutting step of the external shell of the individual cells using blades, followed by different heat treatment processes and stirring processes in an aqueous medium to obtain the cathode with little contamination from the foils, anode material, separator, and electrolyte [18].

### 2.3. Pigment preparation from cathode recovered from LIB waste

A ceramic pigment is usually a metal transition complex oxide obtained by a calcination process which must fulfill three main requirements: (a) thermal stability, maintaining its identity when temperature increases; (b) chemical stability, maintaining its identity when fired with glazes or ceramic matrices; and (c) high tinting strength when dispersed and fired with glazes or ceramic matrices [19].

Due to their composition, active NMC cathode materials recovered from LIBs are prime candidates for the synthesis of some pigments. The Colour Pigments Manufacturers Association (CPMA) establishes a classification of the ceramic pigments following a chemical-structural criteria [20]. Group XIII of the CPMA classification is the most numerous, corresponding to those ceramic pigments with a spinel structure. According to the composition of the cathode recovered, cobalt iron nickel manganese chromium black spinel ((Co, Fe, Ni, Mn) (Fe, Cr)<sub>2</sub>O<sub>4</sub>) was considered a good candidate to be synthesized with this alternative source of raw materials, as it is expected that 100 % of NiO, MnO, and Co<sub>3</sub>O<sub>4</sub> can be provided through the NMC recovered cathode.

The synthesis of the black ceramic pigment (referenced as BP-CAT) consisted of the stoichiometric mixture of the different raw materials in an agate mortar. The mixing of raw materials consisted of 50 wt% of NMC cathode, 10 wt% of Fe<sub>2</sub>O<sub>3</sub>, and 40 wt% of Cr<sub>2</sub>O<sub>3</sub>. Then, the mixture of reagents was introduced in mullite crucibles and calcined in an electric laboratory furnace, using a 10 °C/min heating rate until 1200 °C with a dwell time of 1 h. A standard pigment (referenced as BP-STD) was prepared following the same calcination conditions but using commercial oxides for its formulation, that is, NiO, MnO, Co<sub>3</sub>O<sub>4</sub>, Cr<sub>2</sub>O<sub>3</sub>, and Fe<sub>2</sub>O<sub>3</sub>.

### 2.4. Inkjet ink formulation strategy

Ceramic inkjet inks are made up of complex mixtures consisting, mainly, of a solid constituent comprising (singly or jointly) inorganic pigments/refractory material/ceramic frits, organic solvents, and dispersants [21]. The stability and jettability, the printing resolution, and the layer uniformity deposited onto ceramic substrates are key factors in formulating suitable inks for inkjet printing.

In this context, and in accordance with the specifications and requirements of the technology under consideration, the selection of the different components was influenced by factors such as: chemical compatibility of those with the inkjet system construction components; the chemical nature of both the solid particles and the liquid constituents; the methodology, the temperature, and energy applied during the particle size reduction stage; the evaporation rate of the components at the printhead; and the initial and final particle size and specific surface area of the solid particles.

The preparation of the slurries for inkjet technology was carried out following the subsequent stages.

*Stage 1:* Mixing process combining organic solvents with various additives and solid particles. The slurry was prepared with a 40 % solids content, consisting of a 50:50 mixture of both glycol-ether based solvents, a synthetic polymer dispersant, and the black pigment.

*Stage 2:* Comminution was processed by means of LabStar bead-mill laboratory agitator from Netzsch (to simulate the industrial process), until attaining both a particle size to  $d_{99} < 1.0 \mu\text{m}$  and a filtering capacity of 20 ml through a Sartorius syringe filter of 5  $\mu\text{m}$ . The micronization process was carried out by preparing 6 kg of the test ceramic inkjet ink. The milling was performed using zirconia tetragonal stabilized with Y spheres (average diameter of 300  $\mu\text{m}$ ) as the grinding media. For effective grinding, the volume fraction of the grinding media was 90 % of the volume mill capacity.

*Stage 3:* Verification of the physical properties of the test ceramic inkjet ink: particle size, rheological behaviour and viscosity, density, electrical conductivity, colloidal stability, filtering, and printing capacity. The particle size distribution was determined by laser diffraction using a MASTERSIZER 3000 laser diffraction analyser from MALVERN. The viscosity was conducted using a Brookfield DVE viscosimeter from BROOKFIELD. The density was measured using a DMA 38 densimeter from ANTON PAAR GmbH. The electrical conductivity was carried out using an EC Meter BASIC 30+ conductimeter from CRISON INSTRUMENTS. Finally, experimental printability tests were conducted to evaluate the behaviour of the test ceramic inkjet ink by means of an Inktester from People and Technology, integrated with a XAAR 2001 GS12 piezoelectric printhead, that generates ink drops of approximately 30  $\mu\text{m}$  in diameter. Consistently, a standard “waveform” at 6 kHz was employed, with variations in the electric working voltage. High-resolution images at 720 dpi were reproduced on the ceramic substrates (i.e. single-fired porous and porcelain tiles) to evaluate the technical and aesthetic properties. Fig. 2 shows the design of the printing standards employed in this study.

The firing step was carried out in a laboratory electric furnace using different firing cycles depending on whether the ceramic tile was single-fired porous or porcelain.

### 2.5. Chromatic property analysis

Colorimetric measurements were performed by analyzing the chromatic co-ordinates ( $L^*$ ,  $a^*$ , and  $b^*$ ) using a Macbeth model Colour-Eye 7000A spectrophotometer, a D65 light source, and CIE 10° standard observer according to the Commission Internationale de l’Eclairage (CIE). CIELab system represents the sample colour on a three-



Fig. 2. Printing standards design.

dimensional scale, expressed as brightness  $L^*$ , changing from 0 (black) to 100 (white),  $a^*$  ( $>0$  red,  $<0$  green), and  $b^*$  ( $>0$  yellow,  $<0$  blue).

### 3. Results and discussion

#### 3.1. Cathode characterization

The chemical composition of the NMC cathode recovered is shown in Table 2.

The chemical analysis shows the contamination that the active cathode material undergoes derived from the cutting agents as well as the metallic collectors that support the anode and cathode,  $\text{Cu}^0$  and  $\text{Al}^0$  respectively. This contamination level must be minimized and constant among different batches of NMC cathodes to obtain a by-product that can be used as raw material without causing variations in the final product. Moreover, considerable concentrations of P and F are also present in the composition coming from the electrolyte and binder. The Li values obtained are indicative of a certain level of battery degradation, as the Li content present in cathodes of unused batteries is between the range of 15.5–16.0 wt%. The XRD patterns are given in Fig. 3.

The sample presented very low crystallinity, showing a high degree of degradation. Even though, the characteristic phases of the cathode structure were identified, together with those that are formed due to the degradation process itself, spinel  $\text{Co}_3\text{O}_4$  and rock salt phase  $\text{NiO}$  [22]. Moreover, a little peak of  $\text{CuO}$  was also identified, coming from the current collector at the anode.

The morphology of the particles was also studied by SEM (Fig. 4).

It can be observed that there are two types of particles, ones that are bigger and round, and others that are smaller and more irregular in shape. The spherical particles have a particle size between 5 and 10  $\mu\text{m}$  and consist of granular primary particles, which is the typical morphology of NMC cathodes. The smaller particles may have been generated during the separation process due to the breakage of these spherical particles and they present a particle size below 5  $\mu\text{m}$ .

#### 3.2. Pigment characterization

The chemical composition of the pigments synthesized, both the one with recovered NMC cathode and the standard, is shown in Table 3.

Fig. 5 shows the XRD patterns and aspect of the black pigment synthesized using the NMC cathode recovered from Li-ion batteries as an alternative source of Co, Ni, and Mn.

XRD confirmed the development of the characteristic crystalline

Table 2

Chemical composition of recovered NMC cathode.

| Element (wt%)           |         |
|-------------------------|---------|
| $\text{Co}_2\text{O}_3$ | 53.5    |
| $\text{NiO}$            | 13.3    |
| $\text{MnO}$            | 11.1    |
| $\text{Al}_2\text{O}_3$ | 1.48    |
| $\text{Fe}_2\text{O}_3$ | 2.04    |
| $\text{CaO}$            | 0.11    |
| $\text{MgO}$            | $<0.01$ |
| $\text{Li}_2\text{O}$   | 11.4    |
| $\text{P}_2\text{O}_5$  | 1.03    |
| $\text{CuO}$            | 3.03    |
| F                       | 2.5     |

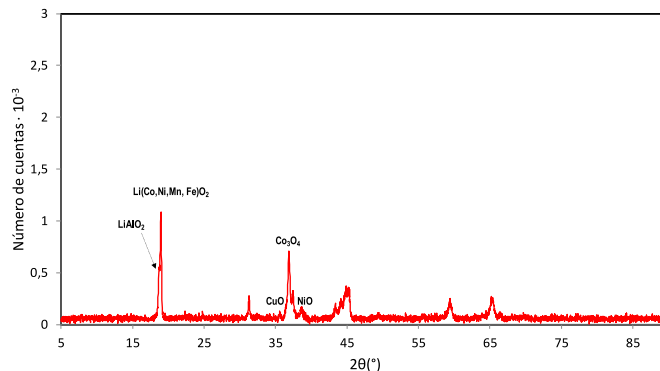


Fig. 3. XRD patterns of recovered NMC cathode.

structure of the pigment selected, that is a spinel structure (Co, Fe, Ni, Mn)  $(\text{Cr,Fe})_2\text{O}_4$ . Besides, a minor phase of spinel  $\text{LiMn}_2\text{O}_4$  was identified which formation is due to the presence of lithium in the composition of the pigment provided by the use of the recovered NMC cathode as alternative raw material.

#### 3.3. Characterization of the test ceramic inkjet ink

Particle size is a critical parameter for ensuring effective inkjet performance within printheads (preventing them from clogging). It is crucial that 99 % of the particles are below 1.0  $\mu\text{m}$ . However, excessive reduction in particle size can lead to ink instability due to particle agglomeration and settling, which may also result in colour loss. Table 4 shows the characteristic diameters of the test ceramic inkjet ink after the comminution stage.

The reduction in size was carried out in two stages: first, the pigment was adapted in a planetary mill to achieve particle sizes below 20  $\mu\text{m}$ , followed by a second milling process using high shear ball milling at 2700 rpm for 110 min.

Viscosity measurements assess the ink performance from storage to its deposition onto a ceramic surface using inkjet technology. The ink is expected to exhibit Newtonian behaviour with relatively low viscosity. Rheological parameters were determined by controlling shear rate and measuring shear stress at 40 °C.

The viscosity results, jointly with density and electrical conductivity data, are detailed in Table 5.

Regarding the density and electrical conductivity of the developments, no significant differences were observed compared to the scientific studies found in the state-of-the-art [23,24], which means that it can be introduced in the same print heads as the conventional inkjet inks. This fact confirms the technical feasibility of reintroducing lithium battery cathodes into the composition of ceramic inkjet inks as an inorganic black pigment.

The final stage of ink characterization involved printing. Before entering the print head, the ink was filtered through a 5  $\mu\text{m}$  membrane. It was subsequently applied to both a single-fired porous tile (fired at a maximum temperature of 1100 °C) and a porcelain tile (fired at a maximum temperature of 1190 °C). This procedure was undertaken both with the inkjet ink formulated with the innovative ceramic pigment (using a ceramic pigment synthesized with the recovered NMC cathode,

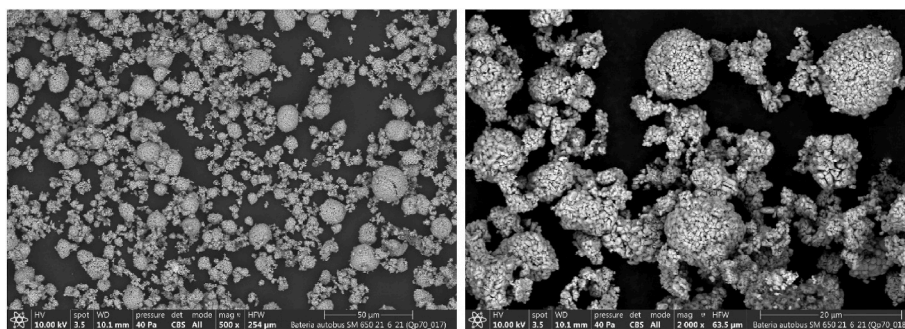


Fig. 4. Morphology of NMC cathode particles (magnification 500x and 2000x).

Table 3

Chemical composition of the pigments synthesized (BP-CST and BP-STD).

| Element (wt%)                  | BP-CAT | BP-STD |
|--------------------------------|--------|--------|
| Cr <sub>2</sub> O <sub>3</sub> | 40.9   | 42.5   |
| CoO                            | 27.5   | 29.6   |
| Fe <sub>2</sub> O <sub>3</sub> | 9.5    | 9.9    |
| NiO                            | 7.3    | 7.8    |
| MnO                            | 7.1    | 7.7    |
| SiO <sub>2</sub>               | 0.7    | 1.2    |
| Al <sub>2</sub> O <sub>3</sub> | 0.8    | 1.0    |
| CaO                            | <0.01  | <0.01  |
| MgO                            | <0.01  | <0.01  |
| Li <sub>2</sub> O              | 3.2    | <0.01  |
| P <sub>2</sub> O <sub>5</sub>  | 0.7    | <0.01  |
| CuO                            | 1.5    | <0.01  |
| F                              | 0.17   | <0.01  |

BP-CAT), and that formulated with the standard pigment (using commercial reagents, BP-STD). Figs. 6 and 7 illustrate the appearance of the tiles after firing.

No defects were observed in either the single-fired porous tile or the porcelain tile, the texture and brightness obtained being appropriate.

The results for the colorimetric parameter measurements are detailed in Table 6.

Slight differences were observed when the samples were fired at different temperatures. Specifically, firing at a higher temperature led to a slight decrease in the brightness ( $L^*$ ) and red hue ( $a^*$ ) values, while the  $b^*$  chromatic coordinate, indicating a blue hue, remained practically unchanged and negative. Consequently, both firing conditions resulted in black colour, with differences imperceptible to visual inspection. Compared to the inkjet ink prepared with the standard pigment, no significant differences were noted, except for a slightly more negative  $b^*$  chromatic coordinate, indicating a slightly bluer hue.

#### 4. Conclusions

The results obtained in this study showed that the cathodes recovered from spent lithium-ion batteries, after suitable separation, could be used as raw materials in the manufacture of ceramic pigments for inkjet applications.

The use of certain virgin raw materials (nickel, cobalt, and manganese oxides specifically) could be reduced or eliminated by their substitution with a recovered cathode of NMC chemistry in the synthesis of certain ceramic pigments, which substitution percentage would depend on the specific composition of the cathode recovered and the type of pigment synthesized.

It was demonstrated that the formation of a secondary spinel due to the presence of lithium in the composition of the cathode recovered did not affect the texture or brightness of the ink once deposited over a ceramic tile and fired (single-fired porous tile and porcelain tile).

These results illustrated the reformation of Li-ion battery waste into ceramic pigments, providing not only waste management benefits for the battery industry but also alternative sources of raw materials for the

Table 4

Values of the characteristic diameters of the test ceramic inkjet ink.

| Characteristic diameters ( $\mu\text{m}$ ) |          |          |          |
|--|----------|----------|----------|
| $d_{10}$                                   | $d_{50}$ | $d_{90}$ | $d_{99}$ |
| 0.169                                      | 0.302    | 0.518    | 0.687    |

Table 5

Viscosity, density, and electric conductivity of the formulated ink.

| Viscosity (40 °C) |        | Density (25 °C) ( $\text{g}\cdot\text{cm}^{-3}$ ) | Electric conductivity ( $\mu\text{S}/\text{cm}$ ) (mPa·s) |
|-------------------|--------|---|---|
| 12 rpm            | 20 rpm |   |   |
| 15.35             | 15.20  | 1.387   | 0.09  |

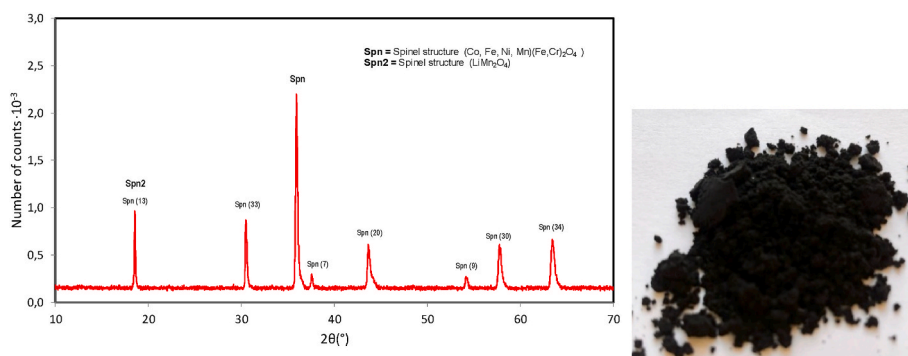


Fig. 5. XRD pattern and aspect of synthesized black pigment.

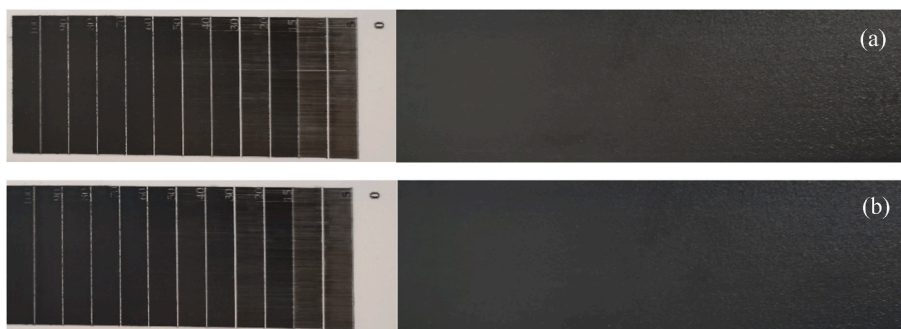


Fig. 6. Design applied over single-fired porous tile (1100 °C): (a) BP-CAT, (b) BP STD.

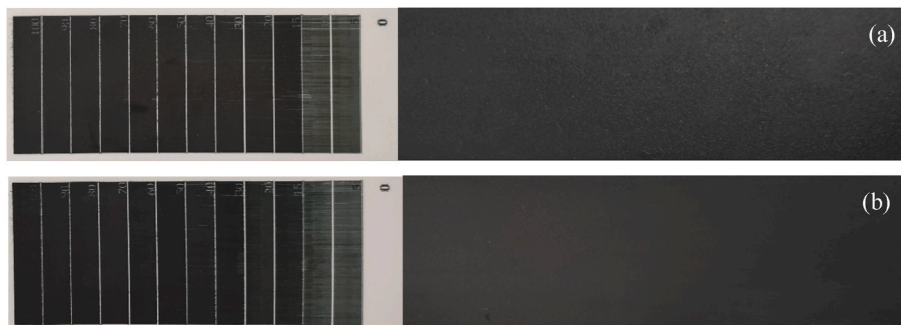


Fig. 7. Design applied over porcelain tile (1190 °C): (a) BP-CAT, (b) BP-STD.

Table 6

CIELab coordinates of the ink deposited over two different substrates fired at different temperature.

|        | T (°C) | L*   | a*   | b*   |
|--------|--------|------|------|------|
| BP-STD | 1100   | 40.3 | -1.1 | -1.8 |
|        | 1190   | 38.9 | -1.4 | -1.9 |
| BP-CAT | 1100   | 40.6 | -1.2 | -2.1 |
|        | 1190   | 38.6 | -1.5 | -2.2 |

ceramic industry.

The introduction of the new black pigment derived from the recovered battery cathode resulted in favourable outcomes in the formulation of a new ceramic inkjet ink. The comminution/milling process and the final physical properties of the formulations confirmed the viability of the proposed separation process. Parameters such as experimental printability enabled the production of decorated ceramic tiles with colorimetric properties comparable to those of inkjet inks formulated from commercial inorganic black pigments.

#### CRedit authorship contribution statement

**Marta Rodrigo:** Writing – review & editing, Writing – original draft, Methodology, Investigation. **María Fernanda Gazulla:** Supervision, Investigation, Funding acquisition. **Eulalia Zumaquero:** Methodology, Investigation. **Jorge González:** Validation, Methodology.

#### Declaration of competing interest

The authors declare that they have no known competing financial interests or personal relationships that could have appeared to influence the work reported in this paper.

#### Acknowledgments

This study was funded by the Generalitat Valenciana, through the

Valencian Institute of Business Competitiveness (IVACE) (grant numbers IMAMCA/2023/1 and IMAMCA/2024/1).

#### References

- [1] S. Chokkha, K. Khaongam, S. Khrongkheha, S. Jankong, N. Chuprasoet, Automotive industrial waste-based pigment synthesis for application in ceramic glaze systems, *J. Mater. Cycles Waste Manag.* 25 (2023) 998–1007, <https://doi.org/10.1007/s10163-022-01581-9>.
- [2] S. Mestre, C. Chiva, M.D. Palacios, J.L. Amorós, Development of a yellow ceramic pigment based on silver nanoparticles, *J. Eur. Ceram. Soc.* 32 (2012) 2825–2830, <https://doi.org/10.1016/j.jeurceramsoc.2011.12.006>.
- [3] SCRREEN, Factsheets updates: cobalt, nickel, manganese. <https://screen.eu/cms-2023/>, 2023. (Accessed 1 July 2024).
- [4] X. Sun, H. Hao, Z. Liu, F. Zhao, Insights into the global flow pattern of manganese, *Res. Pol.* 65 (2020) 101578–101586, <https://doi.org/10.1016/j.resourpol.2019.101578>.
- [5] European Commission, Communication from the commission to the EUROPEAN parliament, the council, the EUROPEAN economic and social committee and the committee of the regions. Critical raw materials resilience: charting a path towards greater security and, Sustainability (2020) 1–24. <https://eur-lex.europa.eu/legal-content/EN/TXT/PDF/?uri=CELEX:52020DC0474>.
- [6] European Commission, Proposal for a REGULATION OF THE EUROPEAN PARLIAMENT AND OF THE COUNCIL establishing a framework for ensuring a secure and sustainable supply of critical raw materials and amending Regulations (EU) 168/2013 (EU) 2018/858, 2018/1724 and (EU) 2019/102, [https://eur-lex.europa.eu/resource.html?uri=cellar:903d35cc-c4a2-11ed-a05c-01aa75ed71a1.0001.02/DOC\\_1&format=PDF](https://eur-lex.europa.eu/resource.html?uri=cellar:903d35cc-c4a2-11ed-a05c-01aa75ed71a1.0001.02/DOC_1&format=PDF), 2023.
- [7] K. Davis, G.P. Demopoulos, Hydrometallurgical recycling technologies for NMC Li-ion battery cathodes: current industrial practice and new R&D trends, *RSC Sust* 1 (2023) 1932–1951, <https://doi.org/10.1039/d3su00142c>.
- [8] J. Xie, Y.-C. Lu, A retrospective on lithium-ion batteries, *Nat. Commun.* 11 (2020) 2499–2502, <https://doi.org/10.1038/s41467-020-16259-9>.
- [9] Battery University, BU-205: types of lithium-ion [on line], [https://batteryuniversity.com/index.php/learn/article/types\\_of\\_lithium\\_ion](https://batteryuniversity.com/index.php/learn/article/types_of_lithium_ion). (Accessed 12 March 2024).
- [10] X. Chen, Y. Chen, T. Zhou, D. Liu, H. Hu, S. Fan, Hydrometallurgical recovery of metal values from sulfuric acid leaching liquor of spent lithium-ion batteries, *Waste Manage. (Tucson, Ariz.)* 38 (2015) 349–356, <https://doi.org/10.1016/j.wasman.2014.12.023>.
- [11] R.-C. Wang, Y.-C. Lin, S.H. Wu, A novel recovery of metal values from the cathode active materials of the lithium-ion secondary batteries, *Hydrometallurgy* 99 (2009) 194–201, <https://doi.org/10.1016/j.hydromet.2009.08.005>.

- [12] McKinsey and Company, Battery 2030: resilient, sustainable, and circular. <https://www.mckinsey.com/industries/automotive-and-assembly/our-insights/battery-2030-resilient-sustainable-and-circular>, 2023. (Accessed 22 November 2023).
- [13] S. Pradhan, R. Nayak, S. Mishra, A review on the recovery of metal values from spent nickel metal hydride and lithium-ion batteries. I, J. Environ. Sci. Technol. 19 (2022) 4537–4554, <https://doi.org/10.1007/s13762-021-03356-5>.
- [14] J. Carneiro, D.M. Tobaldi, R.M. Capela, M.P. Seabra, J.A. Labrincha, Synthesis of ceramic pigments from industrial wastes: red mud and electroplating sludge, Waste Manage. (Tucson, Ariz.) 80 (2018) 371–378, <https://doi.org/10.1016/j.wasman.2018.09.032>.
- [15] M.F. Gazulla, M.J. Ventura, M. Rodrigo, M. Orduña, C. Andreu, E. Zumaquero, From the spent-lithium ion battery to the ceramic pigment, Int. J. Environ. Waste Manag. 33 (1) (2024) 59–73, <https://doi.org/10.1504/IJEW.2024.135877>.
- [16] Regulation (EU) 2023/1542 of the European Parliament and of the Council of 12 July 2023 concerning batteries and waste batteries, amending Directive 2008/98/EC and Regulation (EU) 2019/1020 and repealing Directive 2006/66/EC. <https://eur-lex.europa.eu/legal-content/EN/TXT/?uri=CELEX%3A32023R1542>.
- [17] M.F. Gazulla, M. Rodrigo, M.J. Ventura, J.G. Mallol, M.P. Gómez, J. Gilabert, Direct recycling of lithium-ion cathode: a green solution (applied to laptop batteries), J. Electrochem. Soc. 170 (8) (2023) 80528–80533, <https://doi.org/10.1149/1945-7111/acef5d>.
- [18] Asociación de Investigación de las Industrias Cerámicas AICE, Method for the Recovery of Active Cathode Material from Spent Lithium-Ion Rechargeable Batteries, 2023. Spain Patent No. ES2924113B1).
- [19] G. Monrós, Pigment, ceramic, in: M.R. Luo (Ed.), Encyclopaedia of Color Science and Technology, Springer, New York, NY, 2016, [https://doi.org/10.1007/978-1-4419-8071-7\\_181](https://doi.org/10.1007/978-1-4419-8071-7_181).
- [20] Color Pigments Manufacturers Association, Inc, CPMA Classification and Chemical Description of the Complex Inorganic Color Pigments, 4 ed., 2013. Alexandria.
- [21] G.L. Güngör, A. Kara, D. Gardini, M. Blosi, M. Dondi, C. Zanelli, Ink-jet printability of aqueous ceramic inks for digital decoration of ceramic tiles, Dyes Pigments 127 (2016) 148–154. <https://10.1016/j.dyepig.2015.12.018>.
- [22] Y. Shi, G. Chen, F. Liu, X. Yue, Z. Chen, Resolving the compositional and structural defects of degraded LiNi<sub>x</sub>Co<sub>y</sub>Mn<sub>z</sub>O<sub>2</sub> particles to directly regenerate high-performance lithium-ion battery cathodes, ACS Energy Lett. 3 (2018) 1683–1692, <https://doi.org/10.1021/acseenergylett.8b00833>.
- [23] J. Samuel, P. Edwards, Solvent-based inkjet inks. [https://books.google.es/books?hl=es&lr=&id=awnGCgAAQBAJ&oi=fnd&pg=PA141&dq=Solvent-based+inkjet+inks&ots=KQH9zvRE\\_9&sig=Gw7jxP6O3N70v72WzzYPzOpoLI](https://books.google.es/books?hl=es&lr=&id=awnGCgAAQBAJ&oi=fnd&pg=PA141&dq=Solvent-based+inkjet+inks&ots=KQH9zvRE_9&sig=Gw7jxP6O3N70v72WzzYPzOpoLI), 2009.
- [24] S. Magdassi, The chemistry of inkjet inks. <https://books.google.es/books?hl=es&lr=&id=awnGCgAAQBAJ&oi=fnd&pg=PR5&dq=magdassi+inkjet&ots=KQH9wCQDW5&sig=H3ztMs0KZLwfgBYLNvpzFHZRYiA>, 2009.